The Scattered Disk: Origins, Dynamics and End States

Rodney S. Gomes
Observatório Nacional, Rua General José Cristino 77, CEP 20921-400, Rio de Janeiro, RJ, Brazil

Julio A. Fernández, Tabaré Gallardo
Departamento de Astronomía, Facultad de Ciencias, Iguá 4225, 11400 Montevideo, Uruguay

Adrián Brunini
Facultad de Ciencias Astronómicas y Geofísicas, Universidad de La Plata, Instituto Astrofísico de La Plata, CONICET, Argentina

From a review of the methods that have been used so far, we estimate the present mass of the scattered disk to be in the range 0.01 to $0.1 M_{\oplus}$. We review the dynamics of the scattered disk, paying special attention to the mean motion and Kozai resonances. We discuss the origin of the scattered objects both as coming from the Kuiper belt or as remnants of the scattering process during Neptune's migration. We stress the importance of the mean motion resonance coupled with the Kozai resonance in raising the perihelia of scattered disk objects, emphasizing that fossil and live high perihelion objects could thus have been produced. We analyze other mechanisms that could have implanted the detached scattered objects onto their current orbits, focusing on a few that demand specific explanations. We explore the different end states of scattered disk objects and highlight the importance of their transfer to the Oort cloud.

1. Introduction

The trans-Neptunian (TN) population has a very complex dynamical structure whose details are being uncovered as more trans-Neptunian objects (TNOs) are discovered. At the beginning, two dynamical groups appeared as dominant: (1) the *classical* belt composed of objects in non-resonant orbits with semimajor axes in the range $42 \lesssim a \lesssim 48$ AU in low inclination and low eccentricity orbits; (2) objects in mean motion resonances with Neptune, the *Plutinos* in the 2:3 resonance being the most populous group, which present higher inclinations (Jewitt et al., 1998). Then, object 1996 TL_{66} was discovered belonging to a new category of bodies on highly eccentric orbits, perihelia beyond Neptune ($q > 30$ AU) and semimajor axes beyond the 1:2 resonance with Neptune, here considered for simplicity as $a > 50$ AU (Luu et al., 1997). These bodies were called *Scattered Disk Objects* (SDOs). The sample of discovered SDOs has increased to 96 objects (September 2006). This sample includes several objects with high perihelia (seven objects with $q > 40$ AU). These objects may form one or more sub-populations with respect to their possible origins. These sub-groups have been referred to as high perihelion scattered disk, extended scattered disk, detached objects or inner Oort cloud, this last nomenclature usually associated to the detached objects with the largest semimajor axes (see however Gladman et al., this book, for a review on nomenclature). Although a couple of these objects deserve a specific explanation which is studied elsewhere in this book, we in principle include all of them as SDO's according to the definition above and make a more comprehensive or a more specific analysis wherever suitable throughout this chapter.

From numerical integrations, Levison and Duncan (1997) were able to reproduce such a scattered disk from Kuiper belt objects (KBOs) (or TNOs) strongly perturbed by close encounters with Neptune. According to that work, the scattered disk (SD) would thus represent a transit population from the Kuiper belt to other regions of the solar system or beyond. On the other hand, Duncan and Levison (1997) suggested that the scattered disk could be a relic population of a primordial population of objects scattered by Neptune since the early solar system time. The question is, as we will analyze in this chapter, to what extent a remnant population and a transient population co-exist.

Although it is not an unanimous concept that the objects with $a > 50$ AU and $q > 30$ AU all share the same dynamical origin, we will however adopt this view since it is associated with a quite coherent global dynamical scenario. Since we are mostly concerned with origins we also keep the nomenclature *scattered* instead of *scattering*, this last term suggested in Gladman et al. (this book). Also resonant orbits and those with $e < 0.24$ will be considered globally as scattered orbits provided the basic definition above. Detached objects are here considered basically according to the definition in the chapter by Gladman et al., although we will give special attention to those with $q > 40$ AU.

This chapter is organized as follows. Section 2 describes the orbital configuration of the observed scattered objects and discusses the disk's mass estimate. Section 3 is devoted to the specific dynamics experienced by SDOs. In Section 4, we analyze the processes that could have produced SDO's orbits and draw a conclusion on where most of them

should have come from. The particular sub-population of detached SDOs is studied in Section 5, as to their possible origins. We give special attention to dynamical processes within the known solar system. We also include the dynamical effect of a putative solar companion or rogue planet in driving SDO's perihelia beyond Neptune's neighborhood. For mechanisms that invoke perturbations from an early dense galactic environment, we refer the reader to the chapter by Duncan et al.. In Section 6 we describe three different main end states for scattered disk objects and our review is summarized in Section 7.

2. Orbital Configuration and Mass of the Scattered Disk

Figure 1 plots the different outer solar system populations in the parametric plane semimajor axis vs. perihelion distance. The SDOs occupy the upper right portion of the figure limited by the rightmost full vertical line and the thick dashed horizontal line.

The basic feature in the orbital distribution of scattered objects is that the perihelia are not much beyond Neptune's orbit. This is most likely related to their very origin as discussed in Section 4. Semimajor axes are distributed from just beyond 50 AU to near 500 AU. It is expected that the distribution of semimajor axes shows a concentration (Fig. 1) of objects with relatively small semimajor axes due to the difficulty of observing distant objects. Although SDO's perihelia are usually not much above 30 AU, it is also a remarkable feature that a substantial number of objects do not come closer to the Sun than 36 AU, and very likely a non-negligible fraction of them never comes closer than 40 AU. Above the thinner dashed line in Fig. 1, we see objects belonging to the *Extended Scattered Disk* (Gladman et al. 2002), or, following the nomenclature in Gladman et al. (this book), detached objects with $q > 40$ AU. Although most of them have semimajor axes not much above 50 AU, two of them (Sedna and 2000 CR_{105}) have semimajor axes above 200 AU. These two objects may have had a specific formation process, as addressed in Section 5 (see also Duncan et al., this book). SDOs inclinations can be as low as $0.2°$ or as high as $46.8°$. High inclinations can be attained by close encounters with the planets and/or by the Kozai mechanism inside a mean motion resonance (Section 3).

The population of SDOs with radius $R > 50$ km has been estimated by Trujillo et al. (2000) at $(3.1^{+1.9}_{-1.3}) \times 10^4$ bodies (1 σ errors) and the total mass at 0.05 $M_\oplus$. Trujillo et al. considered the sample of four discovered SDOs at that time, which all had $q \leq 36$ AU. If we consider instead the SDOs up to $q = 40$ AU, Trujillo et al.'s estimate has to be multiplied by at least a factor of two. Therefore, in the following, we will adopt a SD population of $\sim 6 \times 10^4$ objects with $R > 50$ km. An independent survey conducted by Larsen et al. (2001) led to the discovery of 5 Centaurs/SDOs and other two recoveries. From this survey they estimated a population of 70 SDOs brighter than apparent red magnitude $m_R = 21.5$. Applying appropriate

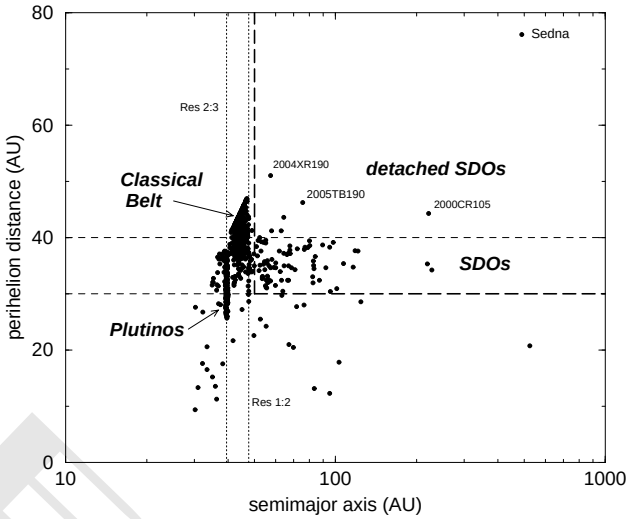

Fig. 1.— Distribution of the different populations of outer solar system bodies in the plane a vs. q. The scattered disk objects occupy the upper right portion of the figure limited by the thick dashed line. The zone of the high-perihelion (or detached) SDOs ($q > 40$ AU) is also indicated and the names of the most prominent members are labeled. The objects were taken from the Minor Planet Center's Web site: http://cfa-www.harvard.edu/iau/Ephemerides/Distant/Soft00Distant.txt.

bias corrections for distance in the detection probability, the estimated total population is in good agreement with that derived above. Trujillo et al. (2001) find that the differential size distribution of classical TNOs follows a power-law $dN \propto R^{-s} dR$, where the index $s = 4.0^{+0.6}_{-1.3}$ (1 σ errors). If we assume that this size distribution also applies to SDOs and that the same exponent s holds down to a typical comet radius $R = 1$ km, the total population of SDOs is estimated to be

$$N_{SDO}(R > 1km) = 6 \times 10^4 \times 50^{(s-1)} \qquad (1)$$

Taking $s = 4.0$ as the most likely value, we obtain $N_{SDO} = 7.5 \times 10^9$, but it may go up to (within 1 σ) 7.8×10^{10}, or down to 1.1×10^9 bodies for $s = 4.6$ and 3.5 respectively. Therefore, there is an uncertainty larger than an order of magnitude in the estimated SD population. A recent deep survey with the HST/ACS camera carried out by Bernstein et al. (2004) suggests a smaller population of small TNOs than that predicted by an extrapolation of a power-law of index $s = 4.0$. The turnover of the size distribution occurs at $D \lesssim 100$ km. The shallower size-distribution for smaller bodies would imply a smaller total mass ≈ 0.01 $M_\oplus$ (Earth masses) for the classical belt, and a mass for the high inclination objects perhaps a few times larger (Bernstein et al., 2004). Yet, Bernstein et al. surveyed a very small sky area of 0.02 deg^2 and discovered only 3 TNOs with diameters between 25 and 44 km (for an assumed albedo 0.04). We have here the problem of small-

number statistics, so these results should be taken with caution.

Delsanti and Jewitt (2006) argue that Trujillo et al.'s (2001) index near 4.0 ± 0.5 for the differential size distribution will slightly flatten towards Dohnanyi's (1969) value of 3.5 due to collisional shattering. Delsanti and Jewitt estimate for the classical disk a mass of a few percent $M_\oplus$ taking into account that large TNOs have high albedos. They also conclude that the mass of the scattered disk should be larger than the mass of the other components of the TN population.

Given the uncertainties, we conclude that the mass of the Scattered Disk might be somewhere in between 0.01 - 0.1 $M_\oplus$, i.e. comparable to the mass of the classical belt. This does not include the mass of objects belonging to the inner core of the Oort cloud, of which Sedna appears to be the most promising candidate (see Section 5).

3. Dynamics of the Scattered Disk

In the trans-Neptunian region the bodies are so weakly linked to the Sun that the osculating heliocentric orbits show important short period oscillations due to the gravitational effects of the giant planets on the Sun. The semimajor axis is the most affected orbital element, oscillating around a mean value that coincides with the barycentric a. For this reason the barycentric orbital elements better represent their dynamical states.

A small body orbiting in the trans-Neptunian region can experience basically two types of dynamical evolutions: a stochastic evolution driven by encounters with the planets and a more regular evolution driven by the continuous and regular gravitational effect due to the planets. The first one, associated with a random evolution of the body's semimajor axis, can only be studied by numerical simulations or by statistical methods but for the second one, which conserves a constant mean value for a, several known results of the secular theory can be applied.

The stochastic evolution of a SDO in general occurs when $q < 36$ AU and is mainly due to encounters with Neptune (Duncan and Levison, 1997; Fernández et al., 2004). In analogy with encounters of comets with Jupiter, after each encounter the SDO's orbital elements should conserve the Tisserand parameter with respect to Neptune:

$$T = \frac{a_N}{a} + 2\sqrt{\frac{a}{a_N}(1-e^2)}\cos i$$

where a_N and a are respectively Neptune's and the body's semimajor axes, e is the body's eccentricity and i its inclination with respect to Neptune's orbit. Strictly speaking, the conservation of T is only valid in the circular 3-body problem, though it may be a good approximation when the object approaches Neptune to less than a few AU. In this case the evolution of the body will proceed stochastically (unless it is in a mean motion resonance), random-walking in the energy space and keeping its perihelion close to Neptune's orbit. However, conservation of T does not apply strictly to the objects with the largest perihelia in the SD, because the gravitational effects of the other giant planets with respect with those of Neptune are no longer negligible. Moreover, if after close approaches to Neptune, the body is transferred inwards, falling under the gravitational influence of Uranus, Saturn or Jupiter, the near constancy of T with respect to Neptune will also break down.

Concerning the more regular evolution, the theory allows us to distinguish here between two kinds of dynamics according to the terms that dominate the Lagrange-Laplace planetary equations (Murray and Dermott 1999). In one case, the evolution is dominated by long period terms that appear in the planetary equations and yields a slow time evolution of the orbital elements, the so–called secular dynamics. In the other case, for specific values of the semimajor axis, a different kind of evolution appears due to long period terms involving mean longitudes λ and λ_N. In this case, we say that the dynamics is dominated by a mean motion resonance (MMR). Once in resonance, the body can experience a secular dynamics, which is in general different from that of non-resonant bodies. We will see below with more details these two types of analytically predictable motions.

3.1. Secular dynamics

For $q \gtrsim 36$ AU, near encounters with the planets are not possible and the object experiences a more regular evolution, very similar to the secular theory predictions. In particular, its barycentric semimajor axis a oscillates around a constant mean value $\overline{a}$ and the longitude of the perihelion ϖ and the longitude of the node Ω have constant rates of precession.

In general, the time evolution of the argument of the perihelion $\omega = \varpi - \Omega$ is a circulation coupled with low amplitude oscillations of e and i. Besides the invariance of $\bar{a}$, the secular evolution imposes the preservation of $H = \sqrt{1-e^2}\cos i$, (when planetary eccentricities and inclinations are neglected), known as Kozai Dynamics (Kozai 1962), and where the inclination is measured with respect to the invariable plane of the planetary system. If $i \simeq 63^\circ$ (also known as *critical inclination*), then $\dot{\omega} \simeq 0$. In this case, ω oscillates. If e is large enough, then high amplitude coupled terms appear in the time evolution of (e, i) (Kozai Resonance). The conservation of H is analogue to the conservation of the Tisserand parameter but the former is a property of the dynamics induced by all the planets and not just by Neptune.

If we consider only this secular evolution, the secular theory tells us that the circulation frequencies of ϖ and Ω in the SD are very small compared with the fundamental frequencies of the solar system, so that no secular resonances (or at least no first order secular resonances) are possible in the SD. Secular resonances occur when the proper frequencies of the SDOs are commensurable with the fundamental frequencies of the planetary system. When the invariable plane of the solar system is used as reference plane instead

of the ecliptic, the fundamental frequencies are related to the circulation frequencies of the elements ϖ and Ω of the planets. For instance, in the classical belt the region between 40 and 42 AU is occupied by the secular resonance ν_8, in which the precession rate of the body's perihelion matches that of Neptune, and ν_{18} which involves the precession of the nodes (Knežević et al. 1991). Secular resonances are important to excite larger eccentricities and inclinations.

Due to the absence of secular resonances the only mechanism that can substantially modify the orbital elements (e, i) of a SDO is the Kozai Resonance (KR) and this occurs only for high-inclination orbits (say $i \gtrsim 50°$) (Thomas and Morbidelli, 1996; Gallardo, 2006a). Then, typical SDOs with perihelion distances $q > 36$ AU and with low inclination orbits would have a stable time evolution with quasi-constant (a, e, i) values provided that the body is outside a MMR. If the body is in a MMR, the KR can occur for much lower inclinations (see below).

3.2. Mean Motion Resonances

Numerical simulations have shown that SDOs, having a stochastic evolution in their semimajor axes, experience temporary captures in high-order MMRs with Neptune (Duncan and Levison, 1997; Gladman et al., 2002; Gomes, 2003; Fernández et al., 2004; Gomes et al., 2005b) suggesting that MMRs can have an important role in the dynamics of the SD. A MMR designed as $|p+q| : |p|$ occurs when the particle's and Neptune's mean motions are commensurable and their locations in barycentric semimajor axis coordinate are given by

$$a_{res} \simeq \frac{a_N}{(1+m_N)^{1/3}} \Big(\frac{p}{p+q}\Big)^{2/3}$$

where m_N is Neptune's mass in solar masses. The integer $q > 0$ is the *order* of the resonance and p is the *degree* which is negative for exterior resonances. All resonances in the SD are exterior to Neptune, then $p < 0$. It is possible to associate a strength to each resonance, which depends on the elements (e, i, ω) of the resonant orbit (Gallardo 2006a, 2006b). They are shown in Fig. 2 for the region between 50 and 150 AU together with the known SD population in that region. The resonance's strength grows with the eccentricity in such a way that, for very high eccentricity orbits, all resonances are strong enough to be relevant. Then, very high eccentricity orbits will be in general affected by a MMR whatever the semimajor axis is.

Using frequency map analysis, Robutel and Laskar (2001) identified several high order exterior MMRs in the region $a < 90$ AU and found the existence of a chaotic region dominated by the superposition of resonances at high eccentricity. They also found that for high inclinations the resonances are wider than for low inclinations. This is in agreement with Gallardo (2006a,b) who finds that, in general, with the exception of Neptune's Trojans and first-order MMRs, resonances are stronger for high inclination orbits.

Gladman et al. (2002) found the empirical result that, for SDOs with $q < 30 + 0.085(a - 30)$ AU and Pluto-like inclination orbits, the dynamics is typically dominated by the mechanism known as *resonance sticking*. This is a dynamical evolution characterized by jumping between different, but near, MMRs that is possible thanks to the superposition of several high order MMRs. In this case the semimajor axis evolves chaotically between resonances but in a very long time scale, so that the body remains essentially confined to semimajor axes $a \lesssim 150$ AU over time scales comparable to the solar system age (see Section 6.2).

A possible mechanism for the capture into a resonant motion is given by the already referred stochastic evolution of the semimajor axis caused by planetary perturbations. Eventually $a \simeq a_{res}$ and the resonant terms of the disturbing function start to dominate the orbital evolution, thus halting the chaotic evolution of a. It must be noted that a MMR offers a natural protection mechanism against close encounters between a pair of bodies. For instance, because Pluto is in the 2:3 MMR resonance with Neptune, the two objects never get closer than about 18 AU to each other, thus preventing Pluto from receiving strong energy kicks during its perihelion passages. If the resonance strength is small, the object will not likely be captured into the resonance since planetary perturbations can overcome the resonance strength and shift a from a_{res}. Resonances of the type 1:n and 2:n with Neptune are relatively strong and isolated from others so they should be the most populated (see Fig. 2). Other resonances could be strong but surrounded by other strong resonances, so the SDO that falls into any of them will evolve by the mechanism of resonance sticking. Table 1 brings a list of the observed SDOs identified in a MMR with Neptune, as coming from a numerical integration based on their nominal orbits. All of them show libration of the critical angle for at least 10^5 yr. The second column is the mean barycentric semimajor axis corresponding to the resonance. Table 1 is in agreement with Table 2 of Gladman et al.'s chapter, which brings a more restricted but more accurate sample of resonant SDOs obtained by a more rigorous process.

Once the SDO is evolving inside an isolated MMR the resonant theory predicts that the body's orbital elements will show very small amplitude oscillations (librations) in (e, i) and somewhat more evident oscillations in a. All these are librating with the same frequency of the critical angle $\sigma = (p+q)\lambda_N - p\lambda - q\varpi$. This is an important difference with respect to librations of asteroids in MMR with Jupiter where the proximity and mass of the planet make the librations' amplitude clearly greater than in the case of resonances with Neptune. But contrary to what we can expect from the theory of the resonant motion, it has been found (Duncan and Levison, 1997) that most commonly the eccentricity and the inclination show notable and slow variations superposed to the almost negligible and relatively quick oscillations due to the resonant motion. This is not due purely to the MMR but also to a secular evolution of the angular element ω that imposes notable excursions of

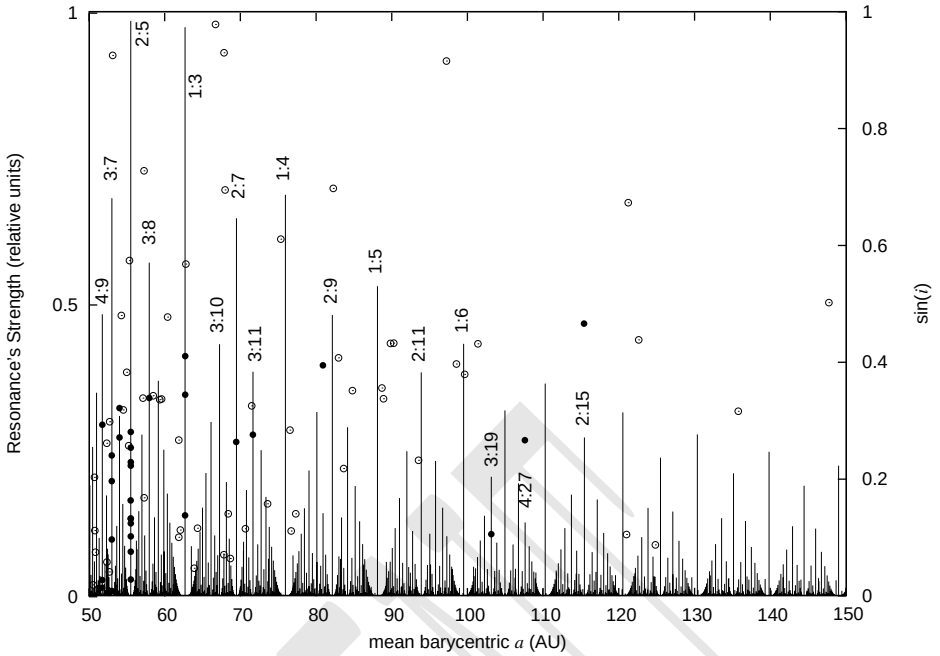

Fig. 2.— Localization and strength of the mean motion resonances in the region $50 < a < 150$ AU. The strengths of all resonances were calculated assuming orbits with $q = 32$ AU, $i = 20^\circ$ and $\omega = 60^\circ$. The known SDOs are plotted in the $(a, \sin i)$ parametric plane in order to appreciate their distribution with respect to the resonance's positions. Full circles indicate objects identified in mean motion resonances with librating critical angles (see Table 1) and open circles indicate objects that were not associated with a resonance. In this plot a is the mean barycentric value after a numerical integration of 10^5 years.

(e, i) (Gallardo, 2006a). These excursions are due to the Kozai Resonance inside the MMR and will be discussed in section 5.1.

Other secular resonances inside a high order MMR with Neptune could occur but this point has not been investigated yet. Three-body resonances involving mean motions of Uranus, Neptune and a SDO are also present in the SD (Morbidelli 2002) and they can possibly contribute to the chaotic evolution of some SDOs but this is not a well investigated issue so far.

4. The Scattered Disk: primordial record or transient population?

We shall discuss now the origin of the SD. One possibility is that it is a byproduct of the formation of the Jovian planets and of the planet migration that was caused by a massive scattering of planetesimals. On the other hand, SDOs may come from the classical belt through processes including collisions (Davis and Farinella, 1997) and a slow diffusion in which mean motion resonances (MMRs) and secular resonances play a fundamental role.

4.1. Migration through a Planetesimal Disk

According to the classical conjecture (Kuiper, 1951), there should be a disk of objects beyond Neptune that, due to its low surface density, could not accrete to form planet-sized bodies. This naturally yields the idea that, at some primordial time, there should have been a disk of planetesimals that extended from the giant planets region up to the putative Kuiper belt outer edge. This orbital configuration of planets and planetesimal disk allows the exchange of energy and angular momentum between particles and planets, at close encounters. This process induces a planetary migration during which Neptune, Uranus and Saturn migrate outwards while Jupiter migrates inwards (Fernández and Ip, 1984; Hahn and Malhotra, 1999). So if we assume that at some time in the past the giant planets coexisted with a disk of planetesimals extending fairly beyond the outermost planet, then we have to conclude that the giant planets were originally on orbits with much smaller mutual separations. The original planetary separations are discussed in several works (Hahn and Malhotra, 1999; Gomes, 2003) and it is possible that Neptune was originally below 20 AU, probably around 15 AU (Gomes, 2003; Tsiganis et al., 2005).

The migration mechanism is fueled by a huge number of close encounters between the planetesimals and the planets. When Neptune reaches the edge of the disk (Gomes et al., 2004) its radial drift is halted (not abruptly but asymptotically). At this point, a great number of planetesimals will be on orbits that already suffered scattering by Neptune, although their cumulative mass is now small enough not to produce any more significant migration of the planet. It is thus a reasonable conclusion that a population of objects scattered by Neptune existed just as the migration calmed down. It is also intuitive to conclude that the present scattered population is composed of those objects that managed to survive up to the present time even though experienc-

TABLE 1
CANDIDATES SDOS IN MMR WITH NEPTUNE

Resonance	a (AU)	Name
4:9	51.72	(42301) 2001 UR_{163}, 2001 KG_{76}, 2001 QW_{297}
3:7	52.99	(95625) 2002 GX_{32}, 2001 XT_{254}, 1999 CV_{118}, 2004 DK_{71}
5:12	53.99	(79978) 1999 CC_{158}, (119878) 2002 CY_{224}
2:5	55.48	(69988) 1998 WA_{31}, (38084) 1999 HB_{12}, (119068) 2001 KC_{77}, (26375) 1999 DE_{9}, (60621) 2000 FE_{8}, 2000 SR_{331}, 2002 GP_{32}, 2002 GG_{32}, 2003 UY_{117}, 2004 EG_{96}, 2001 XQ_{254}
3:8	57.92	(82075) 2000 YW_{134}
1:3	62.65	2003 LG_{7}, 2000 YY_{1}, 2005 EO_{297}
2:7	69.43	2001 KV_{76}
3:11	71.62	(126619) 2002 CX_{154}
5:22	80.88	2004 TF_{282}
3:19	103.10	(29981) 1999 TD_{10}
4:27	107.58	2004 PB_{112}
2:15	115.40	1999 CZ_{118}
1:18	206.87	2002 GB_{32}
4:79	220.07	2000 CR_{105}

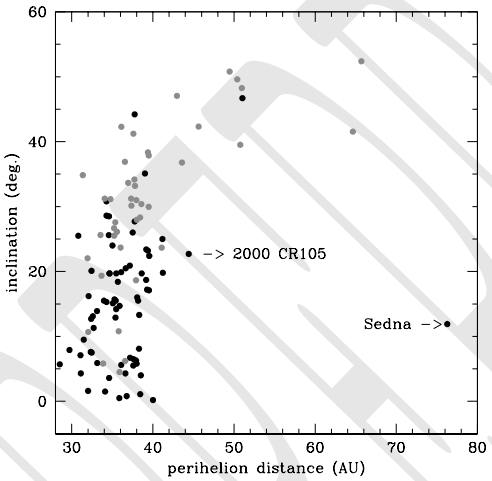

Fig. 3.— Distribution of perihelion distances with inclinations for real scattered objects (black) and objects obtained in a numerical simulation extended to Solar System age (gray). The numerical simulation followed the LHB model (Tsiganis et al. 2005, Gomes et al. 2005a)

ing at some level close encounters with Neptune. In other words, the present scattered objects are the remnants of a much larger scattered population of objects that had perihelia just beyond Neptune's orbit when planetary migration calmed down (Duncan and Levison, 1997).

Estimates of the original planetesimal disk mass range from 50 $M_{\oplus}$ (Hahn and Malhotra, 1999) to 35 $M_{\oplus}$ (Tsiganis et al., 2005; Gomes et al., 2005; Morbidelli et al., 2005). This last number is based on the migration dynamics in a truncated disk that yields good final positions for the giant planets (Tsiganis et al, 2005). Numerical simulations of the migration process extended to the solar system age yield 0.2% to 0.4% (Gomes, 2003; Gomes et al., 2005b) of the original planetesimal disk mass as leftover in the present SD. These simulations also produce a roughly equal number of (hot) classical Kuiper belt objects. A model simulation originally designed to explain the origin of the Late Heavy Bombardment (LHB) on the terrestrial planets (Gomes et al., 2005a), extended for the solar system age, yielded as much as 0.14 $M_{\oplus}$ in the total trans-Neptunian population, with 0.08 $M_{\oplus}$ in the scattered disk. These numbers fairly agree with observational estimates (see Section 2) confirming that the current scattered disk could be produced by the interaction of the primordial planetesimal disk with a migrating Neptune.

Besides the total mass of the scattered disk, it is natural to ask whether the orbital distribution of the SDOs is in agreement with the final outcome of the migration process. As the scattering process proceeds, the average semimajor axis of a body steadily departs from the original value in the proto-planetary disk. However, the semimajor axis is not a good parameter to use for comparisons of simulations with observations, since there must be a great bias in the observational data that favors the discovery of the bodies on the lowest semimajor axes orbits (Morbidelli et al. 2004). Although not quite bias-free, it may be interesting to compare the distribution of perihelion distances and inclinations of the real scattered objects with those coming from a numerical integration extended to the Solar System age. This comparison is shown in Fig. 3 where the black dots refer to the real objects and the gray ones to a numerical integration extended to Solar System age, following the LHB model (Gomes et al. 2005a). It is interesting to note that

both black and gray dots occupy about the same region in the q vs. i parametric space. Sedna is surely a remarkable exception, pointing to another explanation for its origin in addition to the perturbations from the known planets (see Section 5). Although 2000 CR_{105} may have an origin similar to Sedna's (Morbidelli and Levison 2004), this is not clearly concluded from Fig. 3. Another difference between the real and simulated distributions concerns the greater number of low inclination objects in the real population as compared with the simulated one. However this is probably due to observational bias that favors the discovery of low inclination objects.

4.2. From the Classical Kuiper Belt

In the picture outlined before, the present Scattered Disk is the remnant of a much more numerous primordial population, stored on orbits with perihelion distances near Neptune, early in the history of the Solar System.

In this section we will discuss also a possible contribution from the Kuiper Belt to the Scattered Disk, and, more specifically, from the *present* Kuiper Belt to the Scattered Disk.

Duncan et al. (1995) have analyzed the stability of test particles in the TN region. They showed that weak dynamical instabilities are capable of producing an influx of objects from the KB to the SD, and also that the chaotic diffusion in the Kuiper Belt is complex and associated to the superposition of mean motion and secular resonances. In the region occupied by the Plutinos, namely the 2:3 mean motion resonance with Neptune, the instability timescale ranges from less than a million years near the borders of the resonance, to longer than the age of the solar system, deep inside the resonance (Morbidelli, 1997). Performing long-term dynamical simulations of test particles on initially low eccentricity orbits, under the gravitational perturbation of the giant planets, Nesvorný and Roig (2001) also found escape routes from the Kuiper Belt to the Scattered Disk via the chaotic borders of the strong 2:3 and 1:2 mean motion resonances with Neptune, that are known to be occupied by KBOs. They also showed that weaker resonances, such as the 5:7, 8:11, 7:10 and 9:13, are possible routes of chaotic diffusion to the Scattered Disk, and that large eccentricity excitation may also occur for KBOs located at some other high-order resonances with Neptune and three-body resonances with Uranus and Neptune. The region just beyond the 2:3 resonance and up to 43 AU presents a drop in the number of known KBOs. Nesvorný and Roig (2001) computed the maximum Lyapunov Characteristic Exponent of thousands of particles in this region. They have shown that the dynamics is very complex there, and that the characteristic diffusion times are nearly two orders of magnitude shorter than beyond 43 AU. This result was recently confirmed by long-term numerical integrations (Jones et al., 2006). The instability in the $40 - 42$ AU region is due to secular resonances (Duncan et al. 1995).

Lykawka and Mukai (2006) found that inside the 4:7 resonance with Neptune (semimajor axis $a = 43.6$ AU) there are regions of large mobility in phase space, and that bodies inside these regions typically leave the resonance and are subsequently scattered by Neptune. This result is particularly interesting because recent direct numerical integration of trajectories of real KBOs have shown that the 4:7 and 2:5 resonances are inhabited (Chiang et al., 2004).

The chaotic diffusion associated to the resonances has produced a gradual erosion of the primordial Kuiper Belt that continues at present.

In addition, objects inside regions dynamically stable for timescales comparable or even longer than the age of the solar system, can be moved to unstable places in phase space by two mechanisms:

- *Encounters with 1000 km KBOs:* Yu and Tremaine (1999) have shown that Pluto plays some role in shaping the orbital distribution of Plutinos, in the sense that encounters with Pluto can drive some of them out of the 2:3 mean motion resonance. They argued that this mechanism may be a source of Jupiter-family comets. The existence of an object of comparable size within other resonances would have similar significant effects. Nevertheless, none of the 1000 km sized objects known so far in the Kuiper Belt are resonant objects. If any, they await to be discovered.

- *Collisional activity:* The other possibility to populate in a significant way the Scattered Disk from the present Kuiper Belt is via the production of fragments by collisional activity. Davis and Farinella (1997) and Stern and Colwell (1997) have performed the first time-dependent collisional evolution simulations in the Kuiper Belt region. They conclude that the Kuiper Belt is an active collisionally evolved population. Although Chiang et al. (2004) found that no rigorously convincing collisional family can be identified among the non-resonant KBOs they tested, it does not mean that the collisional activity in the Kuiper Belt is not intense, because most collisional families are probably dispersed by the slow chaotic diffusion of the numerous narrow resonances present in the Kuiper Belt (Nesvorný and Roig, 2001). On the other hand Brown et al. (2007) have recently presented dynamical and spectroscopic evidence that the large KBO 2003 EL_{61}, and five other much smaller KBOs, belong to a family that resulted from a near catastrophic collision of the proto-2003 EL_{61}. The typical impact velocity in the Kuiper Belt is 1-2 km s^{-1}, a value that largely exceeds the surface velocity for a typical KBO of size 100-200 km. As a result, Davis and Farinella (1997) estimated that about 10 fragments per year of 1 to 10 km in size are currently produced in the Kuiper Belt region. This number has an uncertainty factor of ~ 4 depending on the assumed collisional response parameter (Davis and Farinella, 1997). The relative velocities of these fragments are enough to change their semimajor axes by

an amount of 0.1-1.0 AU relative to those of their parent bodies. This is sufficient to inject at least a fraction of these fragments into the unstable paths associated to mean motion or secular resonances, and drive them out of the Kuiper Belt. Furthermore, Pan and Sari (2005) argued that KBOs are virtually strengthless bodies held together mainly by gravity (i.e. rubble piles), enhancing the capacity to produce fragments from disruptive collisions, and the flux of them to the Scattered Disk. Yet, we still know very little about the internal strength of KBOs, so we should be very cautious about predictions on collision outcomes

We can conclude that, in addition to the Scattered Disk coming from a primordial scattering process by Neptune, there is a certain flux to the SD of objects coming continuously from the Kuiper Belt, either by dynamical mobility within or near the numerous mean motion resonances or by the injection of small fragments produced in the intense collisional activity that the Kuiper Belt presents.

In a steady state scenario, the mass of the scattered disk objects coming from the Kuiper belt must be a small fraction of that of the KB population. However, observational evidence indicates that the SD and the KB populations have roughly the same mass (cf. Section 2), so we can conclude that most large scattered objects should be remnants of a primordial much larger population scattered by Neptune during its primordial migration. Moreover migration simulations (Section 3.1) roughly reproduce the mass in the SD estimated from observations (Gomes, 2003; Gomes et al., 2005b) and its orbital distribution.

5. The Formation of a High-Perihelion Scattered Disk

There are at present (September/2006) seven objects with $a > 50$ AU and $q > 40$ AU. These are 2003 VB_{12} (Sedna), 2004 XR_{190}, 2004PD_{112}, 2000 CR_{105}, 2000 YW_{134}, 2005 EO_{297} and 2005 TB_{190} (Fig. 1). These objects represent a conspicuous population among the detached objects and will thus be given special attention in this Section. Although it is not unanimous that all detached objects come from the scattered disk we will adopt this view here to be coherent with the scope of this chapter. In the following three subsections we discuss some mechanisms that can raise the perihelia of SDOs and give a tentative classification of each of these seven objects according to its formation mechanism.

5.1. Transfer of SDOs from small q to high q via secular dynamics inside MMRs

Inside a MMR the most important secular effect is the Kozai Resonance which seems to be the rule for resonant orbits with inclinations comparable to that of Pluto, or larger (Gallardo, 2006a). We have stated before that outside a MMR, the KR can only occur at very high inclinations, but inside a MMR the KR can act at lower inclinations. For resonant orbits with Pluto-like or greater inclination, the time evolution of ω slows down, generating non-negligible terms in the resonant equations. These terms cause notable changes of the orbit's (e, i). Figure 4, reproduced from Gomes et al. (2005b) shows a particle that is captured in resonance 1:11 for which almost immediately the KR starts to act. However, for very low inclination orbits, the Kozai Resonance does not appear, so in those cases capture into a MMR is possible, but not associated with strong variations in (e, i).

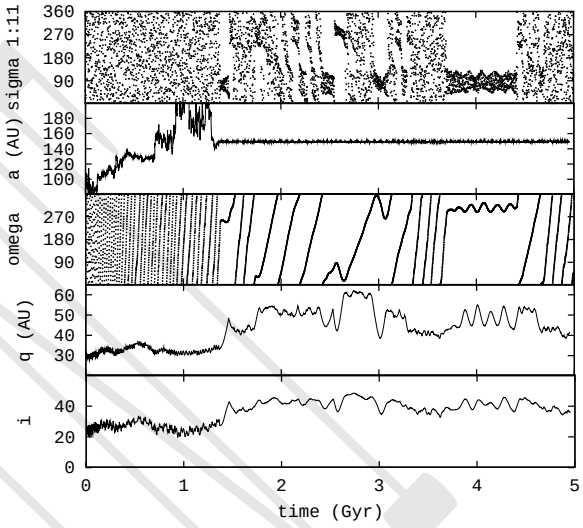

Fig. 4.— Orbital evolution of a test particle captured into the 1:11 resonance and then entering into the Kozai resonance. The test particle is a clone of SDO 1999RZ_{215} (Gomes et al., 2005b).

The coupled MMR+KR mechanism is able to create scattered objects with a quite high perihelion up to ~ 60 AU, as Fig. 4 suggests. Four observed objects with $q > 40$ AU can be associated with this mechanism. These are 2004 XR_{190}, 2000 YW_{134}, 2005 EO_{297} and 2005 TB_{190}. The first one is near the 3:8 mean motion resonance with Neptune, with however a semimajor axis a little smaller than the value corresponding to the resonance center. It is possible that 2004 XR_{190} has escaped the resonance while Neptune was still migrating (see Section 6.1). On the other hand, 2000 YW_{134} is well inside the same 3:8 resonance and is presently experiencing the MMR+KR mechanism (see chapter by Gladman et al.). Numerical integrations of the object 2005 EO_{297} indicate that it is in the 1:3 resonance and could also be experiencing the KR. This can also be the case for 2005 TB_{190} which is near the 1:5 resonance. As seen in Fig. 5, the eccentricity and inclination of a body under the combined effect of a MMR+KR are coupled through the condition $H = \sqrt{1-e^2}\cos i$, where H is constant. This allows us to see what is the minimum perihelion distance allowed for the body and check if it could come from the SD by the MMR+KR mechanism. The answer is negative for 2004 PD_{112}, and also for 1995 TL_8, whose q is 39.986.AU (so, close to our arbitrary boundary

of the detached population, placed at $q = 40$ AU). The origin of these objects is presently obscure but they seem to share the same origin as the cold population in the classical Kuiper belt (see chapter by Morbidelli et al.)

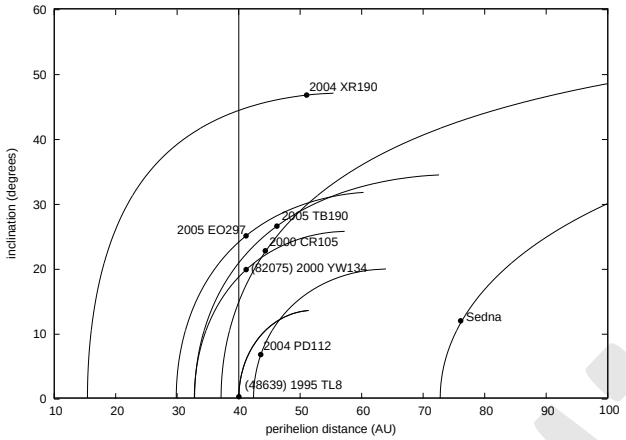

Fig. 5.— Location of seven observed detached objects plus 1995TL8 in the parametric plane (q, i) with the corresponding curves $H = \text{constant}$. These curves show the possible evolution of e and i due to the KR

5.2. Perturbations from external agents

The dynamical mechanism that can raise the perihelia of scattered objects discussed in Section 5.1 can account for many high perihelion orbits of SDOs. Exceptions are, at small a, the low inclination objects, as above commented; at the other extreme, there are two detached objects with large semimajor axes whose orbital origins also cannot be explained by the KR perihelion raising mechanism. One of these is 2000 CR_{105}. It is located at an average distance from the Sun of 221 AU and has a perihelion distance at 44.4 AU. Although numerical integrations may show, at solar system age, objects with semimajor axis and perihelion near 2000 CR_{105} values (Gomes et al., 2005b), the probability of producing objects on orbits with CR105-like perihelion distance but smaller semimajor axis is much larger. This implies that a greater number of CR105-type objects should have been discovered on orbits with smaller a. Furthermore, our numerical experiments also show that the semimajor axes of SDOs with $q > 36$ AU hardly exceeds $a \sim 150$ AU (see Section 6.2 below). Thus one can conclude with some confidence that the mechanism that raised the perihelion of 2000 CR_{105} must be different from the one described in Section 5.1. The second object with large perihelion and semimajor axis is 2003 VB_{12} (Sedna). Its mean barycentric semimajor axis is 505 AU and the object gets no closer to the Sun than 76 AU. Undoubtedly Sedna demands another explanation for its orbit since the mechanism in Section 5.1 cannot explain by no means such a high perihelion. Brown et al. (2004) estimated a total mass of 5 $M_\oplus$ for the population of objects on Sedna-like orbits. This estimate is still highly uncertain because it rests on a single discovery, but it is very likely that Sedna hints at the existence of a substantial population, at least an order of magnitude more massive than that of the Kuiper belt (see chapter by Brown)

Several theories have been proposed to account for Sedna's high perihelion orbit. A theory based on a probable primordial scenario that yields generally good results can be referred to as the 'Sun in a star cluster model' (see Duncan et al., this book). It is based on the assumption that the Sun was formed in a star cluster embedded in a large molecular cloud (Lada and Lada, 2003). This theory considers that objects scattered by the giant planets at the primordial time could have the perihelia lifted through the effect of passing stars and tides from the molecular gas (Fernández and Brunini, 2000; Brasser et al., 2006). It thus generalizes the effect of a single star passage considered in Morbidelli and Levison (2004). The best result is obtained for a cluster with an average density of 10^5 $M_\odot$ pc^{-3} (Brasser et al. 2006). In this case both Sedna and 2000 CR_{105} are well located inside the cluster-produced high-perihelion scattered population.

5.2.1. Perturbations from a solar companion

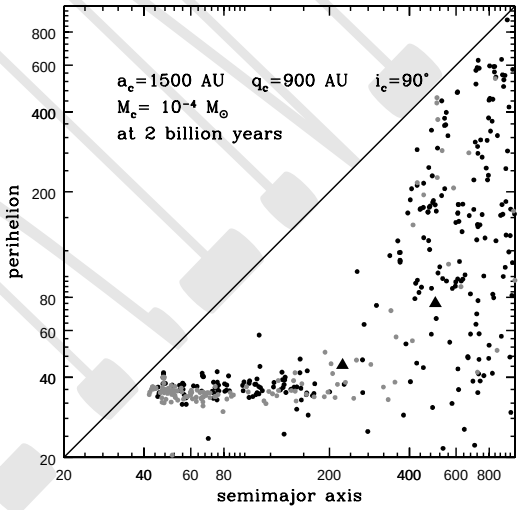

Fig. 6.— Distributions of semimajor axes and perihelia of particles started near Neptune. Direct numerical integration were undertaken with all major planets and a companion with parameters $M_c = 10^{-4}\,\mathrm{M}_\odot$, $a_c = 1500\,\mathrm{AU}$, $e_c = 0.4$ and $i_c = 90^\circ$. Gray dots $\leftrightarrow i < 15^\circ$, black dots $\leftrightarrow i > 15^\circ$, triangles $\leftrightarrow$ Sedna and 2000 CR_{105}.

This section is devoted to a particular mechanism (not included in Duncan et al., this book) that can create very high perihelion orbits from the scattered disk. Perihelion lifting can be experienced by scattered objects through the perturbation of a solar companion (Gomes et al., 2006). This effect is produced by secular and/or Kozai resonances induced by the companion. The precessions of perihelia and

nodes of distant objects are very slow and can often match the precession of the companion's node and perihelion, thus raising secular perturbations. Populations of detached objects, that naturally include Sedna, can be produced by a distant planet orbiting the Sun with semimajor axes ranging roughly from 10^3 to 10^4 AU and masses from a fraction of an Earth mass to several Jupiter masses. There is a relation among semimajor axis, eccentricity and mass of the companion (more concisely semiminor axis and mass) that induces similar orbital distributions for the detached population. This strength parameter is given by $\rho_c \equiv M_c/b_c^3$ where $b_c \equiv a_c\sqrt{1-e_c^2}$ is the companion's semiminor axis and M_c its mass. The companion's inclination also affects the distribution of inclinations of the detached scattered population. In general companions with inclination near 90° create a less inclined extended population. However, numerical simulations show that companions near the solar system invariable plane also induce a low-inclination high-perihelion scattered population. In this case, close encounters with the companion are responsible for lifting the perihelion of several SDOs from Neptune's orbit. Figure 6 shows the distribution of semimajor axes and perihelia, after 2 billion years of integration, of scattered objects, some of which had their perihelia raised by the secular perturbation of a solar companion with $M_c = 10^{-4}$ $M_\odot$, $a_c = 1500$ AU, $q_c = 900$ AU, and $i_c = 90^\circ$. Numerical simulations of a scenario like that of the LHB model (Gomes et al. 2005a) but including also a companion with the same parameters as the one above (except for a 40° orbital inclination), yield a total mass of the detached SDOs of roughly one $M_\oplus$, at solar system age. This is about of the same order of magnitude of the Sedna-like population estimated by Brown et al. (2004).

A basic difference between the star cluster model and the solar companion model is that the latter creates mostly a 'live' population as opposed to the 'fossil' population produced by the star cluster model. The secular effects imposed by the companion continue as long as the companion exists. In this way, objects can move from the scattered disk to the detached population, then back to the scattered disk or they can get a lower perihelion and become *Centaurs*, defined as those objects that cross Neptune's orbit, i.e. that get $q < 30$ AU. Consequently, the influx of comets in the solar companion scenario must be significantly different from those in the no-companion scenario, and this dynamics deserves a specific investigation.

A Jupiter or higher mass companion beyond 5000 AU could have been formed as a small distant binary-star like companion. Relatively smaller companions (Earth to Neptune size at average distances from 10^3 to 2×10^3 AU) could have been scattered by Jupiter or Saturn at very early times of solar system formation and have their perihelia raised by the action of passing starts in a putative dense galactic environment around the primordial Sun, as in the scenario discussed in Section 5.2.

5.2.2. ***Other external perturbations***

Gladman and Chan (2006) present another mechanism, that cannot be strictly classified within the external perturber scenario, but sharing some common features with it. These authors consider that one or more Earth-size bodies were scattered by Neptune in the early solar system, as was previously suggested by Ip (1989) and Petit et al. (1999). From numerical simulations, Gladman and Chan show that a 'rogue' planet interacting with the SDO population, while the planet was still bound to the solar system, would have been able to raise the perihelia of some SDOs to values above 40 AU. This theory is intended to account for the detached objects as a whole but it does not produce detached objects with large semimajor axis like Sedna so effectively as those with smaller semimajor axis.

It is noteworthy mentioning also a mechanism that suggests an extrasolar origin for the large semimajor axis detached objects. As noted above, during the early evolution of the Solar System, the Sun was likely in a dense primordial star cluster. This cluster might contain also substellar objects like brown dwarfs (BDs). If such a BD had an extended planetesimal disk surrounding it, part of this disk could be captured by the Sun during a putative close encounter between the stars, thus producing a population of detached objects including Sedna-like orbits (Morbidelli and Levison 2004; Kenyon and Bromley 2004).The problem with this model is that we do not know if BDs have such extended disks of planetesimals as big as Sedna.

6. End States of Scattered Objects

6.1. A primordial reservoir of detached objects formed by a migrating Neptune

Scattered object orbits are intrinsically unstable by virtue of their very formation process. That is why the current SD population accounts for less than 1% of the original population (Sec. 4.1). Two natural fates for a scattered object can be easily predicted. In fact, Neptune can either scatter out the object by increasing its semimajor axis or it can scatter it into the region with $a < a_N$ if there is a close encounter. The outcomes of these processes are either feeding the Oort cloud or becoming a Centaur and possibly a JFC. These are the subjects of the following two Sections. A third possible fate for a scattered object is obtained if its perihelion is lifted in an irreversible way, so that it enters the detached population and no longer experiences close encounters with Neptune. A fourth less likely fate is the collision with one of the planets (or the Sun).

The mechanisms that induce a perihelion increase by resonant perturbations from Neptune (Section 5.1) has a reversible character so that a high-perihelion scattered object can eventually experience again close encounters with Neptune. The timescale for temporary decoupling from Neptune can be as high as some hundred million years for objects with large semimajor axis (around 200 AU). The irreversibility appears when the conservative character of the

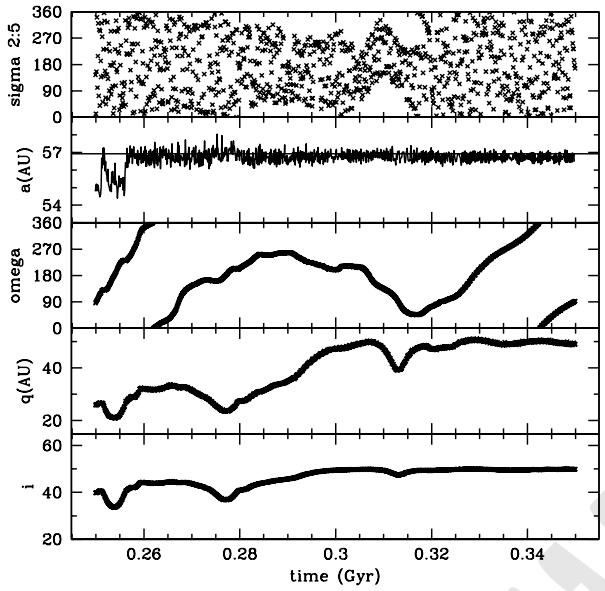

Fig. 7.— Orbital evolution of a SDO captured into the 2:5 MMR with Neptune, also experiencing the Kozai resonance for some time. The particle leaves the 2:5 resonance during Neptune's migration when the eccentricity is low, being fossilized near but outside the MMR.

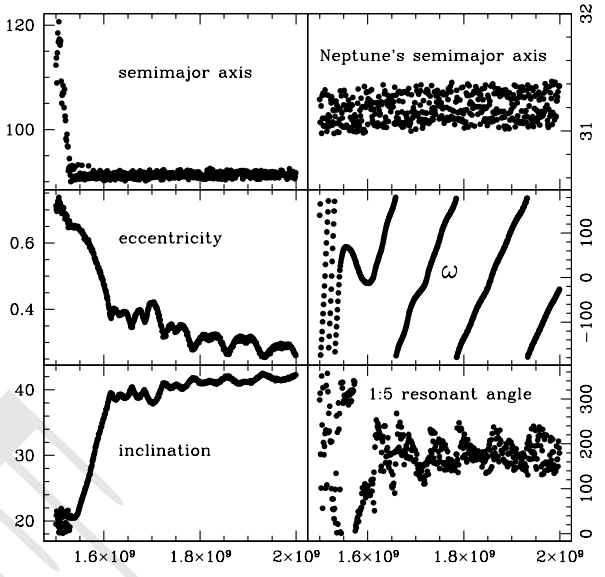

Fig. 8.— Orbital evolution of a SDO captured into the 1:5 MMR with Neptune, also experiencing the Kozai resonance for some time. The particle leaves the Kozai resonance but not the MMR, being fossilized inside the MMR.

planet-particle dynamics is broken by the migration of Neptune or, in other words, by its close interactions with other planetesimals. So, the reservoir of detached objects may be considered as an end state of SDO dynamics given either the irreversibility of the process that increased their perihelion distance or the very long dynamical lifetimes as compared to the solar system age.

Figure 7 shows an example of that dynamical behavior. A scattered object is trapped into the 2:5 resonance with a migrating Neptune. Also experiencing the Kozai resonance inside the MMR, the pair (e, i) starts to follow a variation typical of KR dynamics. At some point when its eccentricity is relatively low and the resonance strength diminishes, the resonance relationship is broken and the particle gets fossilized outside, but in the vicinity of the 2:5 resonance. Another interesting example in shown in Fig. 8. In this case the particle is trapped into the 1:5 resonance with Neptune and starts to experience the Kozai resonance. However, the Kozai resonance is broken when the eccentricity is low but the mean motion resonance keeps active until the end of the integration at 4.5 billion years. In this case, the capture into the MMR and the capture/escape process from the Kozai resonance take place when Neptune migration is very slow. At this point, escapes from the Kozai resonance is possible but escapes from the MMR seem unlikely. For semimajor axis above 100 AU, numerical simulations show trapping into MMR+KR but no escape from any of these resonances seems likely.

During the primordial scattering process, when Neptune still experiences a fairly fast migration, particles are first trapped into the strongest resonances, characterized by small semimajor axes. In this case, escape from the MMR is possible. There must have been a greater fraction of scattered particles with lower semimajor axes as compared with larger semimajor axes in the first hundred million years while Neptune still experienced some migration. This must be responsible for fossilized detached objects outside MMRs, which therefore must be found preferentially at relatively small semimajor axes (say $a < 60 - 70$ AU). The object 2004 XR_{190} may well be a detached object that escaped from the 3:8 MMR with Neptune. A fossil object obtained in a numerical simulation, as shown in Fig. 9, ended at a semimajor axis slightly smaller than that of the 2:5 resonance. 2004 XR_{190} semimajor axis is by a similar amount smaller than that of the 3:8 resonance with Neptune. Inclinations for both 2004 XR_{190} and the simulation object are also of the same order. This suggests that 2004 XR_{190} is a fossil detached object that escaped the 3:8 resonance early in the Solar System evolution when Neptune still experienced migration.

Fossil objects inside a resonance are more likely to be found among middle-valued semimajor axes (say $70 < a < 100$ AU). For larger semimajor axes (say $a > 100$ AU) , numerical simulations show interesting trappings into the mean motion / Kozai resonances with low eccentricity excursions. However in these cases, the particle always gets back to its primordial low perihelion SDO state. Nevertheless, due to the very slow secular evolutions at these remote regions, a particle can show a high perihelion orbit for a

quite long time of the order of several hundred million years (Gomes et al., 2005b).

It is important to note that although we have blamed Neptune's migration for the breakup of a particle's resonance, when its perihelion is high enough, numerical integrations with massless particles (and no induced migration of the planets) also show instances of resonance breakup. When e is low enough, the resonance's strength drops and the resonant relationship can be broken, or at least the libration of the critical angle can be transformed into circulation. At this point the KR stops and only small oscillations in (e, i) coupled with circulation of ω are left. Fig. 10 shows an example where a particle is injected into the high q region due to MMR+KR. Once with high q the resonance's strength, calculated following Gallardo (2006a, 2006b), drops to $1/6$ of its original value and the librations are broken. The object can be stored for billion of years in high q orbits by this mechanism. It must be noted that this is not in a strict sense a case of a dynamical end state since the particle can always return to its original low-q orbit, even though this may take a time longer than the Solar System age. A real end state always needs the action of migration to break the reversibility.

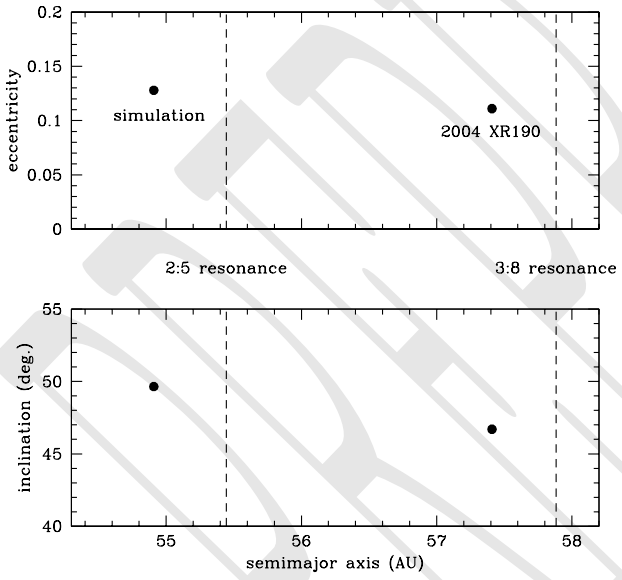

Fig. 9.— Semimajor axis, eccentricity and inclination for an object coming from a numerical simulation (Gomes et al, 2005b) and for 2004 XR_{190}. This figure suggests that, like the simulated object that escaped from the 2:5 resonance, 2005 XR_{190} is a fossil detached object escaped from the 3:8 resonance.

6.2. Feeding the Oort Cloud

SDOs will slowly diffuse outwards under the action of planetary perturbations. We can see in Fig. 11 the dynamical evolution of one of such bodies, 1999 DP_8 that ends up

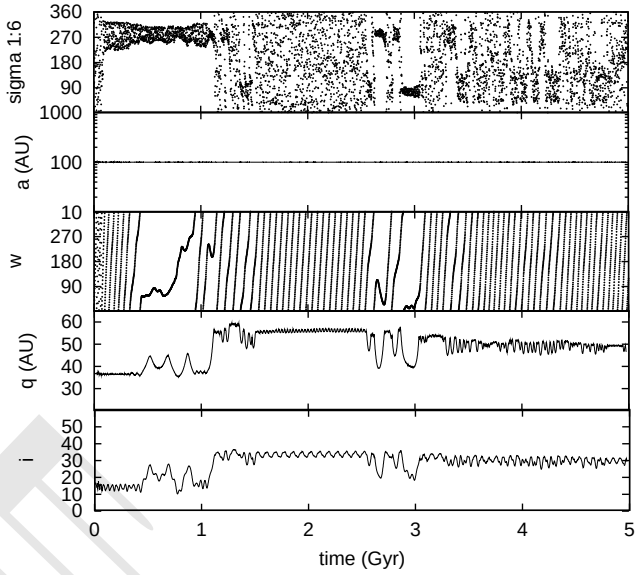

Fig. 10.— An example of particle injected in a high q orbit via MMR+KR and conserved there after the breakup of the resonant motion despite no migration of Neptune occurs in this simulation (Gomes et al. 2005b).

in the Oort cloud after 3.35 Gyr. We note that the Kozai resonance plays a role in the evolution of these bodies, when ω slows down or starts librating around 180°. As seen in the figure, the perihelion distance of the body increases for a while to $q \sim 50$ AU, due to the KR, so that the body avoids close encounters with Neptune. In fact, diffusion of the SDOs in the energy space cannot be described as a random-walk process, since bodies fall very often in different resonances, a process known as resonance sticking as explained before (cf. Section 3.2), which helps to enhance the dynamical longevity of SDOs. The dynamical half-life of SDOs can be expressed as (Fernández et al., 2004)

$$t_{dyn} \simeq 10^{\frac{(q-33.5)}{4.7}} \text{ Gyr} , \qquad (2)$$

where q is expressed in AU. From eq.(2) we get an average lifetime $\bar{t}_{dyn} \sim 1.8 \times 10^9$ yr.

To suffer strong interactions with Neptune, SDOs must first decrease their q to values close to Neptune's orbital radius. At the beginning, a keeps more or less constant as q decreases (thus increasing its eccentricity) (Holman and Wisdom 1993). When SDOs get close to Neptune's orbit they suffer strong perturbations from this planet, so that they can be scattered onto orbits with larger semimajor axes.

Neptune acts as a dynamical barrier that privileges scattering outwards as compared to a slow decrease of the object's perihelion distances near or below Neptune's orbital radius. Fernández et al. (2004) found that about 60% of the bodies inserted in the Oort cloud have perihelia in the range $31 < q < 36$ AU (Fig. 12).

For bodies reaching Neptune-crossing or closely approaching orbits, close interactions with this planet will fa-

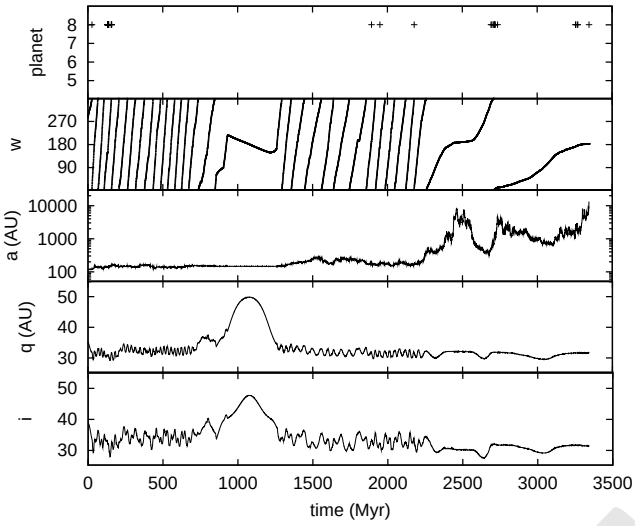

Fig. 11.— Dynamical evolution of the SDO 1999 DP_8 that ends up in the Oort cloud. Close encounters with any of the Jovian planets are indicated in the upper panel, where the numbers 5 .... 8 stand for Jupiter .... Neptune (Fernández et al. 2004).

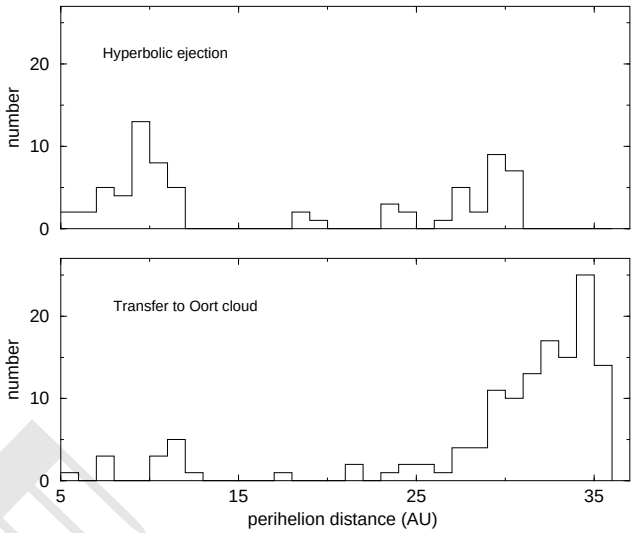

Fig. 12.— The distribution of perihelion distances of a sample of 399 objects, consisting of the real SDOs + clones, at the moment they reach their final states: hyperbolic ejection (upper panel), or insertion in the Oort cloud (lower panel) (Fernández et al. 2004).

vor transfer to the inner planetary region or hyperbolic ejection, instead of insertion into the Oort cloud.

Figure 13 shows the dynamical evolution of fictitious bodies in the parametric plane (a, q). We can see that the transfer to the Oort cloud takes place for bodies with $q < 36$ AU. The sharp upper limit at $q \simeq 36$ AU for bodies diffusing outwards is quite remarkable. We can advance the hypothesis that when SDOs with $q \gtrsim 36$ AU fall in MMRs, planetary perturbations are too weak to dislodge the bodies from such resonances, thus preventing their further evolution in the energy space. Within the MMRs the KR may also act raising the perihelia of the bodies. In such a dynamical state the bodies can be stored for very long time scales.

From the estimated SD population (cf. Sec. 2) and the dynamical lifetime of SDOs, we can compute the current injection rate of SDOs with radii $R > 1$ km into the Oort cloud (Fernández et al. 2004)

$$\nu \simeq \frac{N_{SDO}}{\bar{t}_{dyn}} \simeq 4 \text{ yr}^{-1} \, . \qquad (3)$$

The average rate $\bar{\nu}$ over the age of the solar system should be greater bearing in mind that the primordial SD population could have been up to 10^2 times greater, so a value $\bar{\nu} \sim 10$ should give at least the correct order of magnitude. Adopting this value, we get that the total number of SDOs incorporated into the Oort cloud over the solar system age is $N_{oort} \sim 4.6 \times 10^9 \times 10 = 4.6 \times 10^{10}$. This population has been subject to external perturbers (passing starts, galactic tidal forces) that caused the re-injection of a fraction of it into the planetary region. Most of the objects injected into the planetary region were then ejected to interstellar space.

The previous result shows that the trans-Neptunian belt (via the Scattered Disk) could have been a major supplier of bodies to the cloud, even rivaling other sources within the planetary region, as for instance the Uranus-Neptune zone. And even at present SDOs may still supply the Oort cloud with a significant population.

6.3. Back to the Inner Solar System: Centaurs and JFCs

In addition to the outwards dynamical evolution, SDOs are also able to evolve to the planetary region, becoming Centaurs, and possibly JFCs. Although there is not an unique definition of Centaurs, it is generally accepted that they are objects that enter the planetary region from beyond Neptune (Fernández, 1980; Duncan et al., 1988; Levison and Duncan, 1997). The observed Centaur population, that is strongly biased to low perihelion distances (70% of the known Centaurs have $q < 17$ AU), have a mean lifetime of 9 My (Tiscareno and Malhotra, 2003) with a large dispersion, ranging from 1 My up to lifetimes larger than 100 My. Levison and Duncan (1997), through numerical simulations, estimated the number of JFCs with $H_T < 9$ ($R \gtrsim 1$ km) as 1.2×10^7. Sheppard et al. (2000), conducted a wide-field CCD survey for Centaurs. They concluded that if the differential size distribution is a power law with $s \sim 4$, and assuming an albedo of 0.04, the number of Centaurs should be of the order of 10^7. Therefore, assuming that the population of Centaurs is in steady state, the rate of injection of Centaurs from the Scattered Disk would be of ~ 1 object larger than 1 km per year (assuming that the SD is the source of all Centaurs).

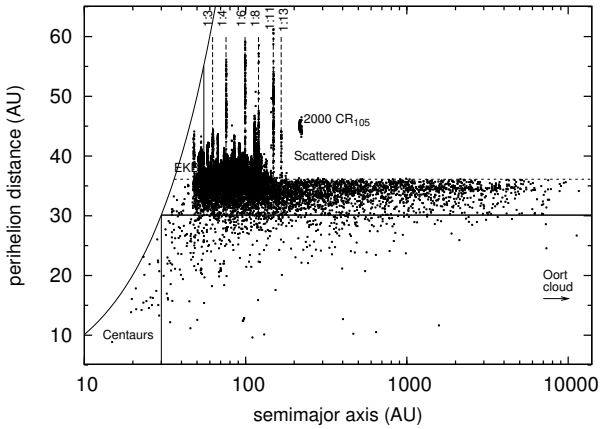

Fig. 13.— Perihelion distance versus semimajor axis of all the objects (real SDOs + clones) plotted every 50 Myr (Fernández et al. 2004).

7. Conclusions

The best estimate for the scattered disk mass is in the range 0.01 to 0.1 $M_\oplus$, thus comparable to the Kuiper belt mass. Due to our poor knowledge of the albedo and size distribution of the SDOs, the SD mass cannot be more precisely determined.

Most SDOs must be relics from a much more numerous population of objects, scattered from a primordial disk by Neptune during its migration. However, some SDOs may have escaped from the Kuiper belt by some chaotic dynamical process. Since SDOs very frequently fall in MMRs, due to resonance sticking, their diffusion in the energy space cannot be properly described as a random-walk. We note that in the region $a < 200$ AU no objects with $q > 36$ AU are found to diffuse to the Oort cloud in timescales of Gyrs. In a MMR, a SDO may experience also the Kozai resonance inducing an important increase of its perihelion distance, temporarily detaching the objects from Neptune's close perturbation. If this mechanism takes place while Neptune is still migrating, fossil detached objects can be created, by the rupture of the reversibility of the resonant dynamics. Sedna and possibly 2000 CR_{105} could not have their perihelia increased by the sole effect of the known planets. An external agent is needed to detach these objects from Neptune's close influence. The formation of the Sun in a dense star cluster could have raised the perihelia of distant detached objects like Sedna. A solar companion at roughly 10^3 AU to 10^4 AU from the Sun with a mass from an Earth mass to several Jupiter masses can also raise the perihelia of scattered objects, thus producing a 'live population' of detached objects that naturally includes Sedna and 2000 CR_{105}.

Neptune constitutes a dynamical barrier that prevents most SDOs to diffuse inwards. This privileges the outwards scattering of SDOs that eventually feed the Oort Cloud. There may be still at present a significant contribution of SDOs to the Oort cloud. However, some SDOs may nevertheless escape to the solar system inside Neptune's orbit becoming a Centaur or possibly a Jupiter family comet.

Acknowledgments. R.G. acknowledges financial support by CNPq, J.A.F. and T.G. from CSIC, and A.B. from ANPCyT. We thank V. Emel'yanenko for reviewing this chapter. We are indebted to A. Morbidelli for his many comments and suggestions to improve this chapter.

REFERENCES

Bernstein, G.M., Trilling, D.E., Allen, R.L., Brown, M.E., Holman, M., and Malhotra, R. 2004. The size distribution of trans-Neptunian bodies. *Astron. J. 128*, 1364-1390.

Brasser, R., Duncan, M.J. and Levison, H.F. 2006. Embedded star clusters and the formation of the Oort cloud *Icarus 184*, 59-82.

Brown, M.E., Trujillo, C., and Rabinowitz, D. 2004. Discovery of a candidate inner Oort cloud planetoid *Astrophys. J. 617*, 645-649.

Brown, M.E., Barkume, K.M., Ragozzine, D., and Schaller, E.L. 2007. Discovery of an icy collisional family in the Kuiper belt. *Nature*, in press.

Chiang, E.I.,Lovering, J.R., Millis, R.L. et al. 2004. Resonant and secular families of the Kuiper Belt. *Earth, Moon and Planets 92*, 49-62.

Davis, D.R., and Farinella, P. 1997. Collisional evolution of Edgeworth-Kuiper Belt objects. *Icarus 125* 50-60.

Delsanti, A., and Jewitt, D. 2006. The solar system beyond the planets. In *Solar System Update* (Ph. Blondel, and J. Mason, Eds.), pp. 267-294, Springer-Praxis, Germany.

Dohnanyi, J.W. 1969. Collisional models of asteroids and their debris. *J. Geophys. Res. 74* 2531-2554.

Duncan, M.J., and Levison H.F. 1997. A disk of scattered icy objects and the origin of Jupiter-family comets. *Science 276*, 1670-1672.

Duncan, M.J., Levison H.F., and Budd, S.M. 1995. The dynamical structure of the Kuiper belt. *Astron. J. 110*, 3073-3081.

Duncan, M., Quinn T., and Tremaine S. 1988. The origin of short-period comets. *Astrophys. J. Lett. 328*, L69-L73.

Fernández, J.A. 1980. On the existence of a comet belt beyond Neptune. *Mon. Not. R. Astr. Soc. 192*, 481-491.

Fernández, J.A., and Brunini A. 2000. The buildup of a tightly bound comet cloud around an early Sun immersed in a dense Galactic environment: Numerical experiments *Icarus 145*, 580-590.

Fernández, J.A., Gallardo T., and Brunini A. 2004. The scattered disk population as a source of Oort cloud comets: evaluation of its current and past role in populating the Oort cloud. *Icarus 172*, 372-381.

Fernández, J.A., and Ip, W.-H. 1984. Some dynamical aspects of the accretion of Uranus and Neptune: the exchange of orbital angular momentum with planetesimals. *Icarus 58*, 109-120.

Gallardo, T. 2006a. The occurrence of high order mean motion resonances and Kozai mechanism in the scattered disk. *Icarus 181*, 205-217.

Gallardo, T. 2006b. Atlas of mean motion resonances in the solar system. *Icarus 184*, 29-38.

Gladman, B., Holman, M., Grav, T., Kavelaars, J., Nicholson, P., Aksnes, K., and Petit, J.-M. 2002. Evidence for an extended scattered disk. *Icarus 157*, 269-279.

Gladman, B., and Chan C. 2006. Production of the extended scattered disk by rogue planets. *Astrophys. J. 643*, L135-L138.

Gomes, R.S. 2003. The origin of the Kuiper belt high-inclination population. *Icarus 161*, 404-418.

Gomes, R.S., Morbidelli, A., and Levison, H.F. 2004. Planetary migration in a planetesimal disk: why did Neptune stop at 30 AU? *Icarus 170*, 492-507.

Gomes, R.S., Levison, H.F., Tsiganis, K. and Morbidelli, A. 2005a. Origin of the cataclysmic Late Heavy Bombardment period of the terrestrial planets *Nature 435*, 466-469.

Gomes, R.S., Gallardo, T., Fernández, J.A., and Brunini, A. 2005b. On the origin of the high-perihelion scattered disk: the role of the Kozai mechanism and mean motion resonances *Celest. Mech. Dyn. Astron. 91*, 109-129.

Gomes, R.S., Matese, J., and Lissauer, J. 2006. A distant planetary-mass solar companion may have produced distant detached objects *Icarus 184*, 589-601.

Hahn, J.M., and Malhotra, R. 1999. Orbital evolution of planets embedded in a planetesimal disk. *Astron. J., 117*, 3041-3053.

Holman, M.J., and Wisdom, J. 1993. Dynamical stability in the outer Solar System and the delivery of short period comets. *Astron. J. 105*, 1987-1999.

Ip, W.-H. 1989. Dynamical processes of macro-accretion of Uranus and Neptune: A first look. *Icarus 80*, 167-178.

Jewitt, D.G., Luu, J., and Trujillo, C. 1998. Large Kuiper belt objects: The Mauna Kea 8K CCD survey. *Astron. J. 115*, 2125-2135.

Jones, D.C., Williams, I.P., and Melita, M.D. 2006. The dynamics of objects in the inner Edgeworth-Kuiper Belt. *Earth, Moon and Planets* , in press.

Knežević, Z., Milani, A., Farinella, P., Froeschle, Ch. and Froeschle, Cl. 1991. Secular resonances from 2 to 50 AU. *Icarus 93*, 316-330.

Kenyon, S.J., and Bromley, B.C. 2004. Stellar encounters as the origin of distant Solar System objects in highly eccentric orbits. *Nature 432*, 598-602.

Kozai, Y., 1962. Secular Perturbations of Asteroids with High Inclination and Eccentricity. *Astron. J. 67*, 591-598.

Kuiper, G. 1951. On the origin of the solar system, in: Hynek, J.A. (Ed.), Astrophysics: A Topical Symposium, McGraw-Hill, New York, pp. 457-414.

Lada, C.J., and Lada, E.A. 2003. Embedded Clusters in Molecular Clouds. *Annual Review of Astronomy & Astrophysics 41* 57-115.

Larsen, J.A., Gleason, A.E., Danzi,N.M., Descour, A.S., McMillan, R.S., Gehrels, T., Jedicke, R., Montani, J.L., and Scotti, J.V. 2001. The Spacewatch wide-area survey for bright Centaurs and trans-Neptunian objects. *Astron. J. 121*, 562-579.

Levison, H.F., and Duncan, M.J. 1997. From the Kuiper belt to Jupiter-family comets: The spatial distribution of ecliptic comets. *Icarus, 127*, 13-32.

Luu, J., Marsden, B.G., Jewitt, D., Trujillo, C.A., Hergenrother, C.W., Chen, J., and Offutt, W.B. 1997. A new dynamical class of object in the outer Solar System. *Nature 387*, 573-575.

Lykawka, P.S., and Mukai T. 2006. Exploring the 7:4 mean motion resonance - II: Scattering evolutionary paths and resonance sticking. *Planet. Space Sci. 54* 87-100.

Morbidelli, A. 1997. Chaotic diffusion and the origin of comets from the 2/3 resonance in the Kuiper belt. *Icarus 127*, 1-12.

Morbidelli, A. 2002. Modern Celestial Mechanics. Ed. Taylor & Francis.

Morbidelli, A., and Levison, H.F. 2004. Scenarios for the Origin of the Orbits of the Trans-Neptunian Objects 2000 CR105 and 2003 VB12 (Sedna) *Astron. J. 128*, 2564-2576.

Morbidelli, A., Emelyanenko, V.V., and Levison, H.F. 2004. Origin and orbital distribution of the trans-Neptunian scattered disc *MNRAS 355*, 935-940.

Murray, C.D., and Dermott, S.F., 1999. Solar System Dynamics. Cambridge University Press, Cambridge, UK.

Nesvorn'y, D., and Roig, F. 2001. Mean motion resonances in the trans Neptunian region. Part II: 1:2, 3:4 and weaker resonances. *Icarus 150*, 104-123.

Pan, M., and Sari, R. 2005. Shaping the Kuiper Belt size spectrum by shattering large but strengthless bodies. *Icarus 173*, 342-348.

Petit, J.-M., Morbidelli, A., and Valsecchi, G.B. 1999. Large scattered planetesimals and the excitation of the small body belts. *Icarus 141*, 367-387.

Robutel, P., and Laskar, J. 2001. Frequency map and global dynamics in the solar system I. *Icarus 152*, 4-28.

Sheppard, S.S., Jewitt, D.C., Trujillo, C.A., Brown, M.J.I., and Ashley, M.C.B. 2000. A wide-field CCD survey for centaurs and Kuiper belt objects. *Astron. J. 120*, 2687-2694.

Stern, S.A., and Colwell, J.E. 1997. Accretion in the Edgeworth-Kuiper belt: Forming 100-1000 km radius bodies at 30 AU and beyond. *Astron. J. 114*, 841-849.

Thomas, F., and Morbidelli, A., 1996. The Kozai resonance in the outer solar system and the dynamics of long-period comets. *Cel. Mech. Dyn. Ast. 64*, 209-229.

Tiscareno, M.S., and Malhotra, R. 2003. The dynamics of known Centaurs. *Astron. J., 126*, 3122-3131.

Trujillo, C.A., Jewitt, D.C., and Luu, J.X. 2000. Population of the scattered Kuiper belt. *Astrophys. J. 529*, L103-L106.

Trujillo, C.A., Jewitt,D.C., and Luu, J.X. 2001. Properties of the trans-Neptunian belt: Statistics from the Canada-France-Hawaii telescope survey. *Astron. J., 122*, 457-473.

Tsiganis, K., Gomes, R.S., Morbidelli, A., and Levison, H.F. 2005. Origin of the orbital architecture of the giant planets of the Solar System. *Nature 435*, 459-461.

Yu, Q., and Tremaine, S. 1999. The dynamics of plutinos. *Astron. J. 118*, 1873-1881.